Supporting Information

A tetranuclear Ni^{II}-Mannich base complex with oxygenase, water splitting and ferro and antiferromagnetic coupling properties

Arka Patra,[a] Avijit Das,[b] Abhimanyu Sarkar,[b] Carlos J. Gómez-García,[c] Chittaranjan Sinha*[a]

[a,b]*Department of Chemistry, Jadavpur University, Kolkata-700032, India. email:crsjuchem@gmail.com*

[c]*Departmento de Química Inorgánica. Universidad de Valencia, C/ Dr. Moliner 50, 46100 Burjasot (Valencia) Spain.*

Characterization of H_2L and compound 1

Elemental analyses (C, H and N) have been performed using a Perkin Elmer 2400 series II CHN analyser. The FT-IR spectra were recorded at ambient temperature in the range 400-4000 cm^{-1} with a Perkin Elmer SPECTRUM II LITA FT-IR spectrometer. Electronic spectra were collected in methanol solutions in the range 800-200 nm using a Perkin Elmer Lambda 35 UV/Vis Spectrophotometer. Electrospray ionization mass spectrometry (ESI-MS positive) was performed with a Xevo G2-S QT of (Waters) mass spectrometer, equipped with a Z-spray interface spectrometer. The X-band EPR spectra were measured using a Bruker ELEXSYS 580 spectrometer in methanol at 110 K.

Variable temperature magnetic susceptibility measurements were performed in the temperature range 2-300 K with an applied magnetic field of 0.1 T on a polycrystalline sample of compound **1** with a mass of 24.931 mg, using a Quantum Design MPMS-XL-5 SQUID susceptometer. The susceptibility data were corrected for the sample holder previously

measured using the same conditions and for the diamagnetic contribution of the sample, as deduced by using Pascal's constant tables.[1]

Crystallographic data collection and refinement

Single crystals of the ligand, H_2L and compound **1** were mounted on glass fibres. Intensity data were collected on a Bruker-AXS SMART APEX II CCD diffractometer equipped with a mono-chromated Mo-Kα (λ = 0.71 Å) radiation source with the ω/2θ scan technique at 298 K. The crystal structures were solved with the SHELXS 2016/6,[2] SHELXL 2018/3,[3] and PLATON 99[4] structure solution. The structure of compound **1** contains solvent-accessible voids, which has been treated using Olex2.[5] Data collection, structure refinement parameters and crystallographic data for the ligand and the compound **1** are shown in **Table 1**. The CCDC numbers **2298689** (H_2L) and **2298690** (compound **1**) contain the supplementary crystallographic data for this work. Selected bond distances and angles for the ligand H_2L are displayed in **Tables S1** and **S2**, respectively and for compound **1** in **Tables S3** and **S4**, respectively. H-bonds in compound **1** are displayed in **Table S5**.

Table S1. Selected bond lengths (Å) in the ligand **H_2L.**

Atoms	Distance (Å)	Atoms	Distance (Å)	Atoms	Distance (Å)
O1-C1	1.362(2)	O2-C2	1.369(3)	O2-C7	1.414(3)
N1-C9	1.468(3)	N1-C10	1.469(3)	N1-C11	1.469(2)
C4-C5	1.385(3)	C3-C4	1.393(3)	C2-C3	1.378(3)
C4-C8	1.512(3)	C5-C6	1.391(3)	C6-C9	1.514(3)

Table S2. Selected bond angles (°) in the ligand **H_2L**.

Atoms	Angle (°)	Atoms	Angle (°)	Atoms	Angle (°)
C2-O2-C7	117.51(18)	C9-N1-C10	111.86(17)	C9-N1-C11	110.85(17)

C10-N1-C11	109.09(15)	O1-C1-C2	117.32(19)	O1-C1-C6	123.07(17)
C2-C1-C6	119.59(19)	O2-C2-C1	114.84(18)	O2-C2-C3	125.13(18)
C1-C2-C3	120.0(2)	C2-C3-C4	121.21(19)	C3-C4-C5	118.0(2)

Table S3. Selected bond lengths (Å) in compound **1**.

Atoms	**Distance (Å)**	**Atoms**	**Distance (Å)**	**Atoms**	**Distance (Å)**
Ni1-O3	2.125(6)	Ni1-O9	2.297(7)	Ni1-O10	2.153(6)
Ni1-O14	2.119(6)	Ni1-N1	2.086(7)	Ni1-N2	2.116(8)
Ni2-O5	2.025(6)	Ni2-O7	2.058(6)	Ni2-O11	2.252(8)
Ni2-O12	2.146(7)	Ni2-N3	2.110(7)	Ni2-N4	2.116(7)
Ni3-Cl1	2.281(4)	Ni3-Cl2	2.088(6)	Ni3-O3	2.015(6)
Ni3-O7	2.022(6)	Ni3-O8	2.104(6)	Ni3-O13	2.131(7)
Ni4-Cl1	2.249(4)	Ni4-Cl2	2.087(6)	Ni4-O4	2.124(7)
Ni4-O5	2.014(6)	Ni4-O6	2.153(6)	Ni4-O14	2.002(6)

Table S4. Selected bond angles (º) in compound **1**.

Atoms	**Angle (º)**	**Atoms**	**Angle (º)**	**Atoms**	**Angle (º)**
O3-Ni1-O9	85.3(2)	O3-Ni1-O10	81.4(2)	O3-Ni1-O14	110.5(2)
O3-Ni1-N1	90.4(3)	O3-Ni1-N2	159.5(3)	O9-Ni1-O10	160.0(2)
O9-Ni1-O14	86.3(2)	O9-Ni1-N1	94.5(3)	O9-Ni1-N2	102.1(3)
O10-Ni1-O14	84.5(2)	O10-Ni1-N1	100.4(3)	O10-Ni1-N2	95.5(3)
O14-Ni1-N1	159.1(3)	O14-Ni1-N2	89.2(3)	N1-Ni1-N2	70.1(3)
O5-Ni2-O7	108.1(2)	O5-Ni2-O11	85.5(3)	O5-Ni2-O12	84.4(2)
O7-Ni2-O12	85.9(2)	O7-Ni2-N3	91.7(3)	O7-Ni2-N4	160.5(3)

O5-Ni2-N3	159.5(3)	O5-Ni2-N4	90.2(3)	O7-Ni2-O11	83.1(3)
O12-Ni2-O11	162.0(3)	N3-Ni2-O11	102.6(3)	N3-Ni2-O12	91.9(3)
N3-Ni2-N4	71.0(3)	N4-Ni2-O11	91.7(3)	N4-Ni2-O12	103.1(3)
Cl2-Ni3-Cl1	91.8(2)	O3-Ni3-O13	80.1(2)	O3-Ni3-O8	93.4(2)
O7-Ni3-O13	93.2(3)	O7-Ni3-O8	78.8(2)	O8-Ni3-O13	88.9(3)
Cl2-Ni4-Cl1	92.8(2)	Cl2-Ni4-O6	170.2(2)	O4-Ni4-Cl1	172.7(2)
O5-Ni4-O6	78.5(2)	O14-Ni4-O4	79.2(2)	O14-Ni4-O5	168.0(3)
O14-Ni4-O6	93.2(3)	Ni4-Cl1-Ni3	83.23(14)	Ni4-Cl2-Ni3	92.2(2)
Cl1-Ni3-O3	94.6(2)	Cl1-Ni3-O7	92.6(2)	Cl1-Ni3-O8	170.8(2)
Cl2-Ni3-O8	92.3(3)	Cl2-Ni3-O13	173.2(3)	O3-Ni3-O7	169.9(2)
Cl1-Ni3-O13	88.1(2)	Cl2-Ni3-O3	93.1(2)	Cl2-Ni3-O7	93.6(2)
Cl1-Ni4-O5	93.9(2)	Cl1-Ni4-O6	87.5(2)	Cl1-Ni4-O14	94.4(2)
Cl2-Ni4-O4	91.4(3)	Cl2-Ni4-O5	91.7(2)	Cl2-Ni4-O6	170.2(2)
Cl2-Ni4-O14	96.6(2)	Ni3-O3-Ni1	118.7(3)	O4-Ni4-O6	89.5(3)
O3-Ni1-O9	85.3(2)	O3-Ni1-O10	81.4(2)	O3-Ni1-O14	110.5(2)
O3-Ni1-N1	90.4(3)	O3-Ni1-N2	159.5(3)	O9-Ni1-O10	160.0(2)
O9-Ni1-O14	86.3(2)	O9-Ni1-N1	94.6(3)	O9-Ni1-N2	102.1(3)
O10-Ni1-O14	84.5(2)	O10-Ni1-N1	100.4(3)	O10-Ni1-N2	95.5(3)
O14-Ni1-N1	159.1(3)	O14-Ni1-N2	89.2(3)	N1-Ni1-N2	70.2(3)
O5-Ni2-O7	108.1(2)	O5-Ni2-O11	85.6(3)	O5-Ni2-O12	84.4(3)
O7-Ni2-O12	85.9(2)	O7-Ni2-N3	91.7(3)	O7-Ni2-N4	160.5(3)
O5-Ni2-N3	159.5(3)	O5-Ni2-N4	90.2(3)	O7-Ni2-O11	83.1(3)
Cl1-Ni3-O3	94.6(2)	Cl1-Ni3-O7	92.7(2)	Cl1-Ni3-O8	170.8(2)
Cl2-Ni3-O8	92.2(3)	Cl2-Ni3-O13	173.2(2)	O3-Ni3-O7	169.9(3)

Cl1-Ni3-O13	88.1(2)	Cl2-Ni3-O3	93.1(2)	Cl2-Ni3-O7	93.6(2)
Cl1-Ni4-O5	93.9(2)	Cl1-Ni4-O6	87.5(2)	Cl-Ni4-O14	94.4(2)
Cl2-Ni4-O4	91.4(3)	Cl2-Ni4-O5	91.7(2)	Cl2-Ni4-O6	170.2(2)
Cl2-Ni4-O14	96.6(2)	O4-Ni4-O5	92.0(3)	O4-Ni4-O6	89.5(3)

Table S5. List of H-bonding interactions in compound **1**.

D-H···A	D-H (Å)	H···A (Å)	D···A (Å)	D-H-A (°)
O10-H10B···Cl1	0.91	2.06	2.794(8)	137
O12-H12A···Cl1	0.81(5)	2.42(6)	3.078(8)	139(9)
O9-H9B···Cl2	0.90	2.40	3.000(8)	125
O11-H11A···Cl2	0.84(5)	2.03(5)	2.817(10)	156(8)
O12-H12A···Cl3[1]	0.83(5)	2.38(6)	3.152(7)	154(7)
O10-H10A···Cl3[2]	0.91	2.40	3.148(7)	139
O9-H9A···Cl4	0.89	2.18	2.839(7)	130
O11-H11B···Cl4[2]	0.84(6)	2.54(8)	3.218(9)	139(9)

1 = x, y,1+z; 2 = 2-x,1/2+y,1-z

Table S6. Continuous SHAPE measurement values of the five possible coordination geometries with coordination number six[34] for the four nickel centres in compound **1**. Lower values are indicated in bold.

Geometry	Symmetry	Ni1	Ni2	Ni3	Ni4
HP-6	D_{6h}	34.462	32.924	31.629	31.750
PPY-6	C_{5v}	19.925	21.084	26.802	26.573
OC-6	**O_h**	**3.208**	**3.017**	**0.720**	**0.805**
TPR-6	D_{3h}	8.022	7.504	14.275	13.884
JPPY-6	C_{5v}	24.710	25.491	30.770	30.468

HP-6 = Hexagon, PPY-6 = Pentagonal pyramid, OC-6 = Octahedron, TPR-6 = Trigonal prism and JPPY-6 = Johnson pentagonal pyramid J2.

Catalytic oxidation of 3,5-DTBC and *o*-aminophenol

Compound **1** was used as a catalyst for the oxidation of of 3,5-DTBC (3,5-di-tert-butylcatechol) and *o*-aminophenol (OAP). A methanolic solution of **1** (10^{-4} M) was treated with 100 eq. of a methanolic solution of 3,5-DTBC or OAP (10^{-2} M) under aerobic conditions at 27°C, to investigate catecholase-like and phenoxazinone synthase-like activities, respectively. After the addition of the substrate to the solution of **1**, the reaction progress was monitored by recording the UV-Vis spectra of the mixture at 3-minute time intervals. The gradual increment in the absorption bands observed around 408 and 425 nm indicates that compound **1** catalyses the aerobic oxidation of 3,5-DTBC to 3,5-DTBQ and 2-Aminophenol (OAP) to 2-aminophenoxazin-3-one (APX), respectively. Generation of H_2O_2 throughout the reaction had been estimated via the generation of I^- oxidation to I_3^- by spectrometric technique in case of catecholase like activity.[6]

The kinetic parameters for the oxidation were determined from the value of the slope of the absorbance *vs*. time plot from the initial 5 minutes (the molar extinction coefficient of the 3,5-DTBQ and APX moieties are taken as 1630 and 9300 M^{-1} cm^{-1} at λ = 408 and 425 nm, respectively. The experimental rate *vs*. concentration of the substrate was found out using the Michaelis-Menten method to get the Lineweaver-Burk diagram and to estimate the kinetic parameters V_{max}, K_M and k_{cat} of compound **1**, where V_{max} = maximum rate achieved by the compound **1**; K_M = Michaelis constant and k_{cat} = catalytic efficiency (**Table S7**). The catalytic efficiencies(**k_{cat}**) are compared with those reported for other transition metal complexes (**Tables S8 and S9**).

Iodometric Method for the determination of I_3^-. We used the iodometric method to find evidence of hydrogen peroxide formation during the catalytic reaction. First, the reaction mixture was created by mixing compound 1 with 3,5-DTBC in 1:100 ratio. Following a one-

hour reaction, H_2SO_4 was added to the solution to acidify it until the pH of the solution became 2. An equivalent amount of water was added to stop additional oxidation, and the resulting quinone was extracted three to four times using dichloromethane. One millilitre (10%) of KI solution and three drops of 3% ammonium molybdate solution were added to the aqueous layer. The spectrophotometric monitoring of the $\mathbf{I_3^-}$ formation was made possible by the development of the distinctive $\mathbf{I_3^-}$ band[6] (λ = 353 nm, ε = 26000 M^{-1} cm^{-1}).

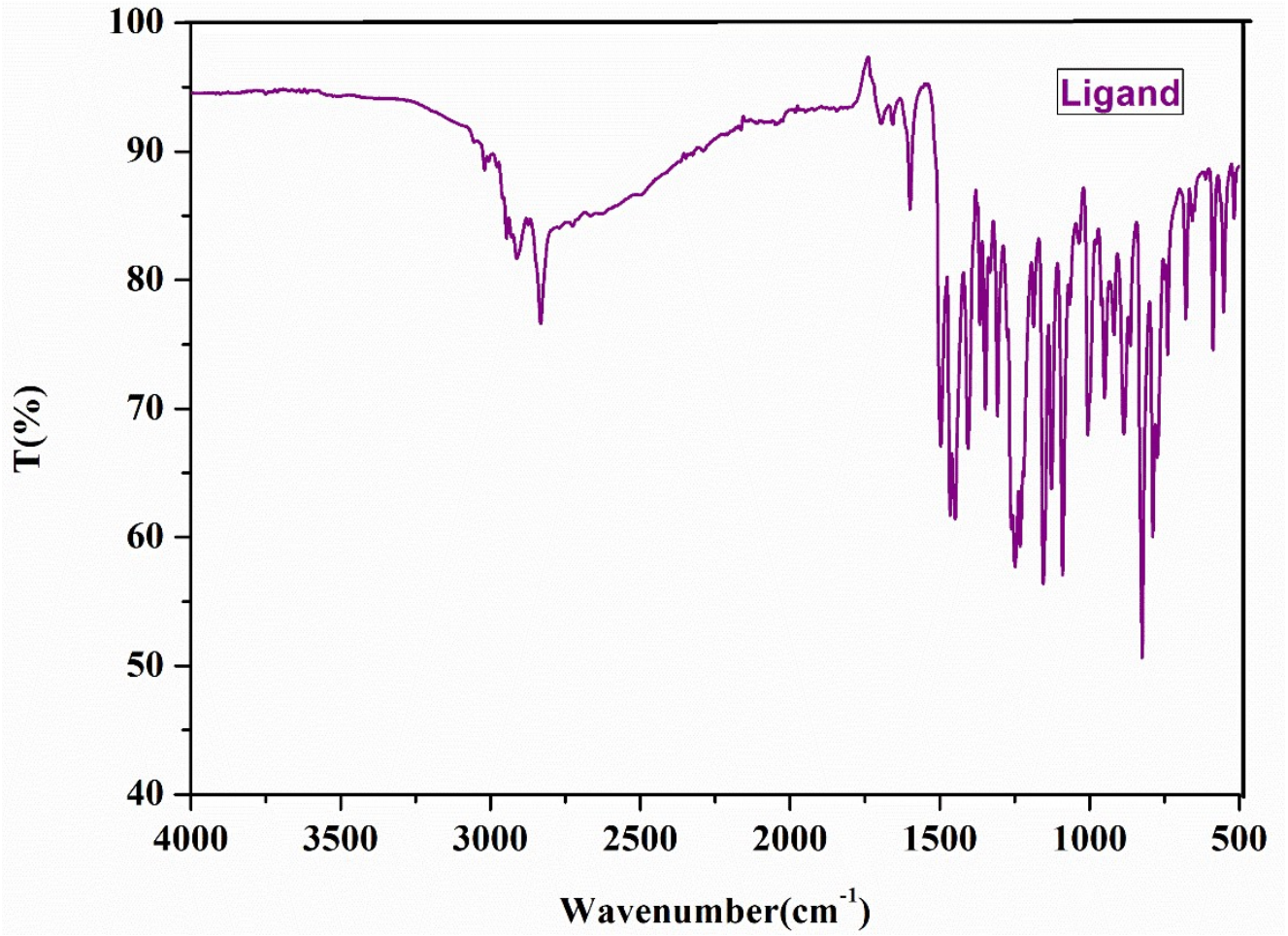

Fig. S1. IR spectrum of the ligand H_2L.

Fig. S2. Mass spectrum of the ligand H_2L in CH_3OH solvent.

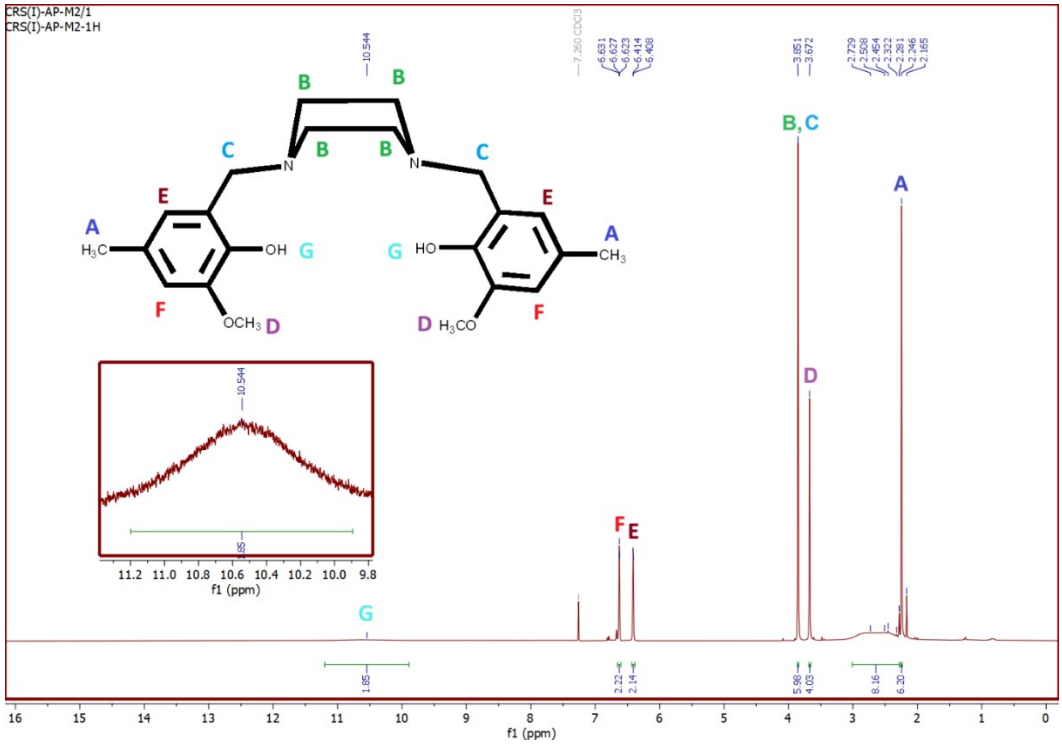

Fig. S3. ^{1}H NMR spectrum of ligand H_2L in $CDCl_3$

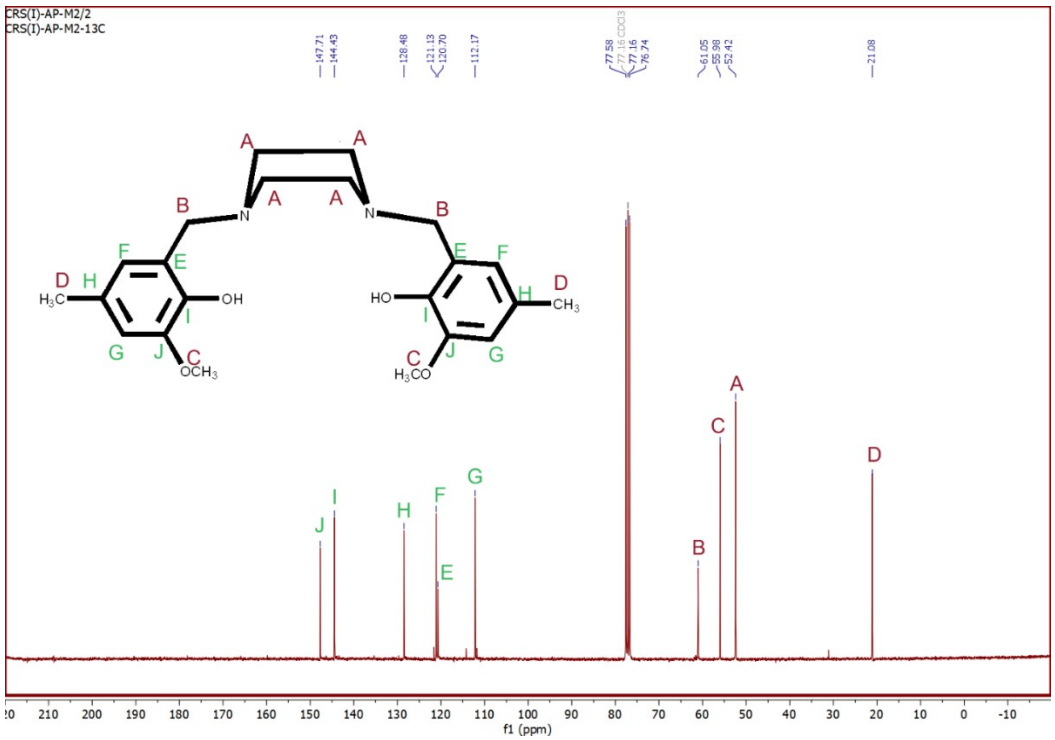

Fig. S4. ^{13}C NMR spectrum of ligand, H_2L in $CDCl_3$.

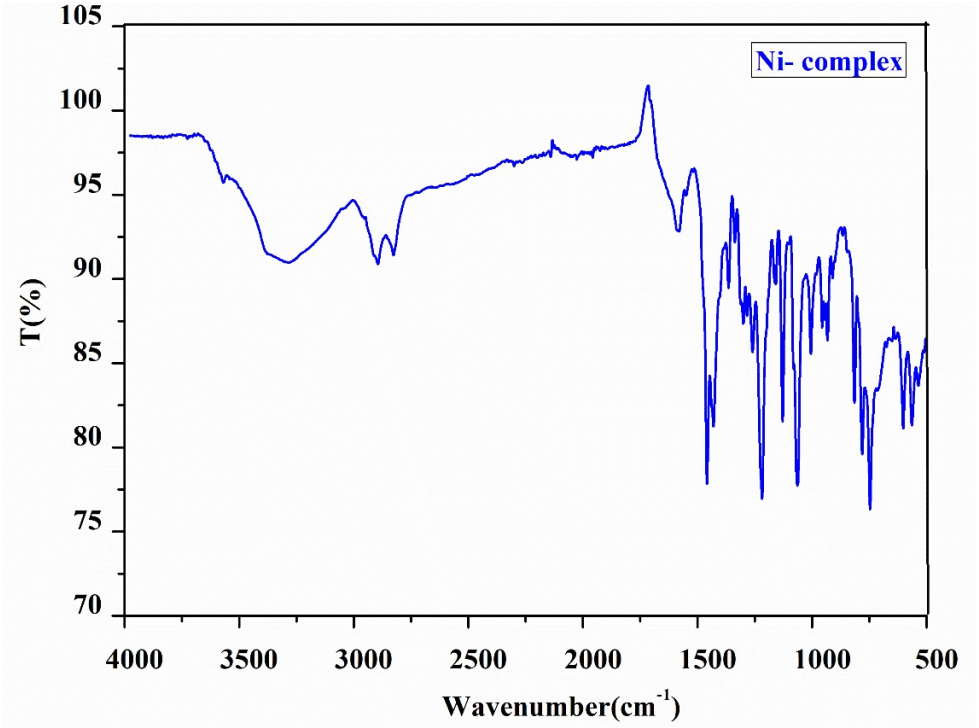

Fig. S5. IR spectrum of compound **1**.

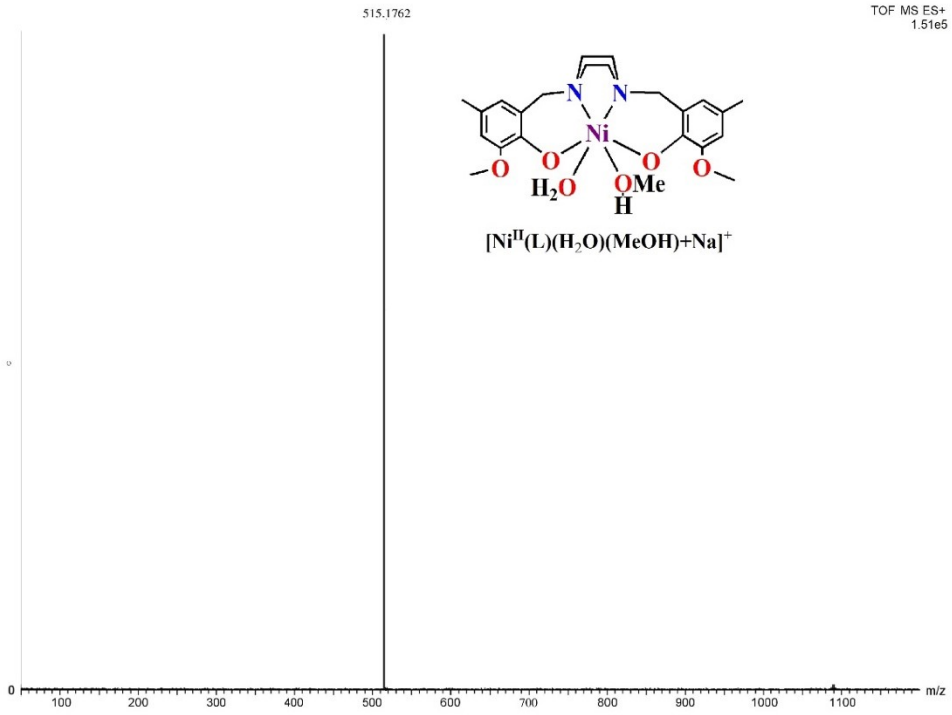

Fig. S6. Mass spectrum of compound **1** in CH_3OH.

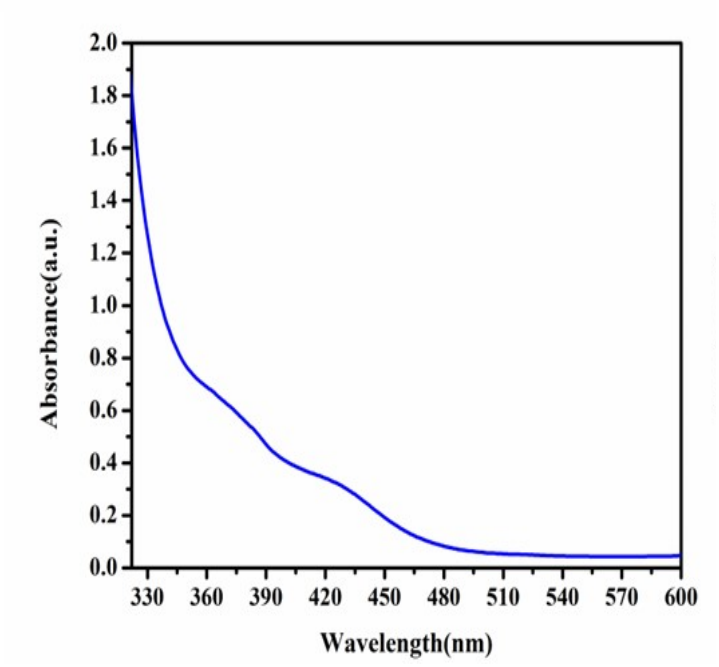

Fig. S7. UV-Vis spectrum of compound **1** in methanol.

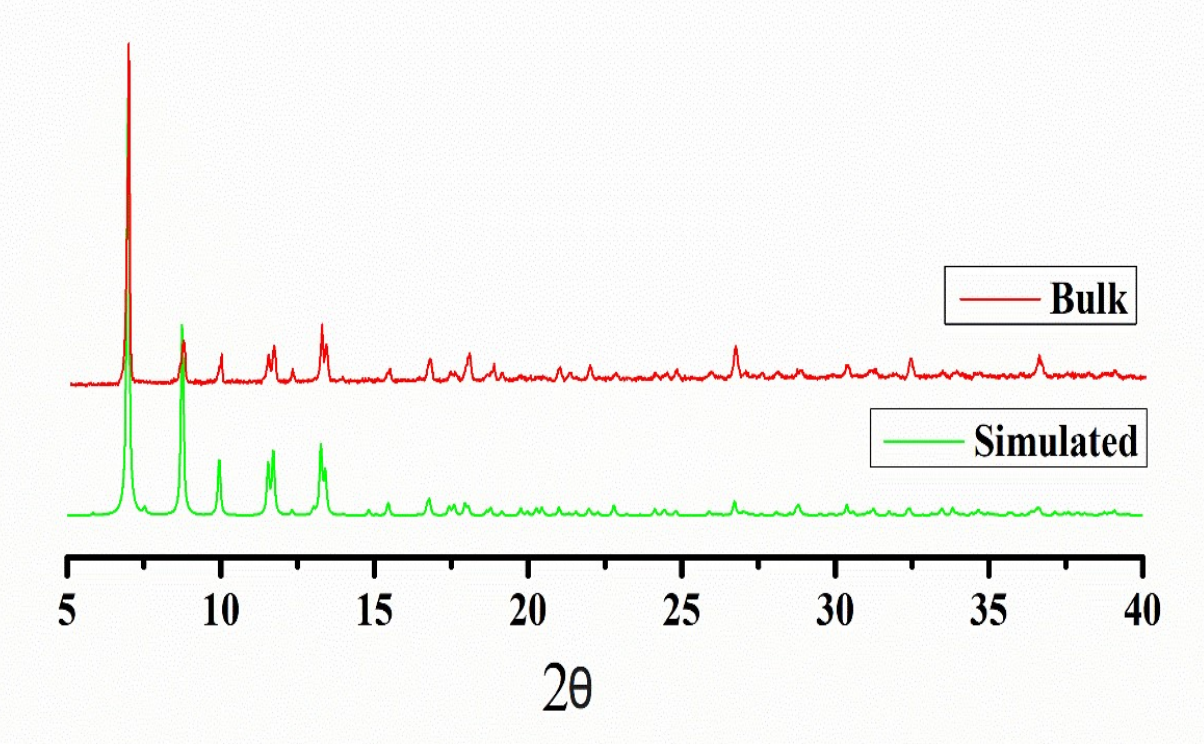

Fig. S8. Powder XRD data of compound **1**

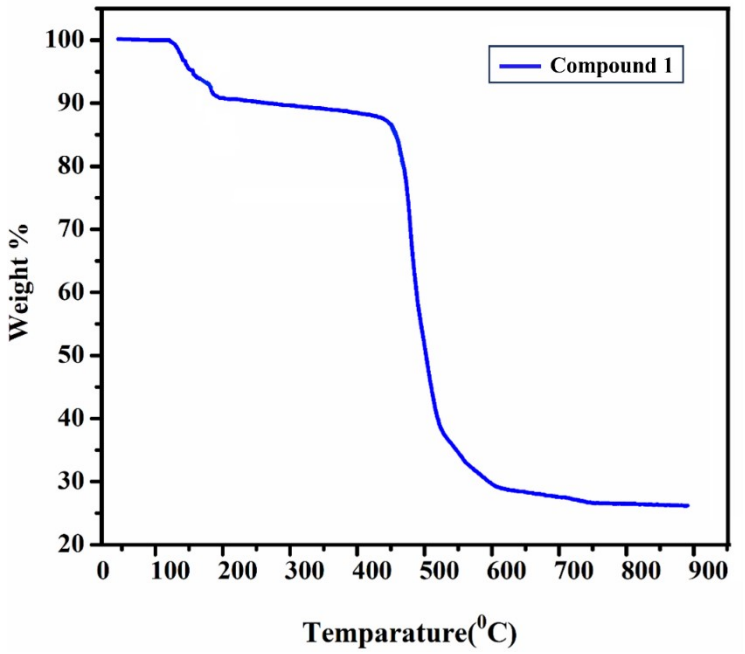

Fig. S9. Thermogram of compound **1.**

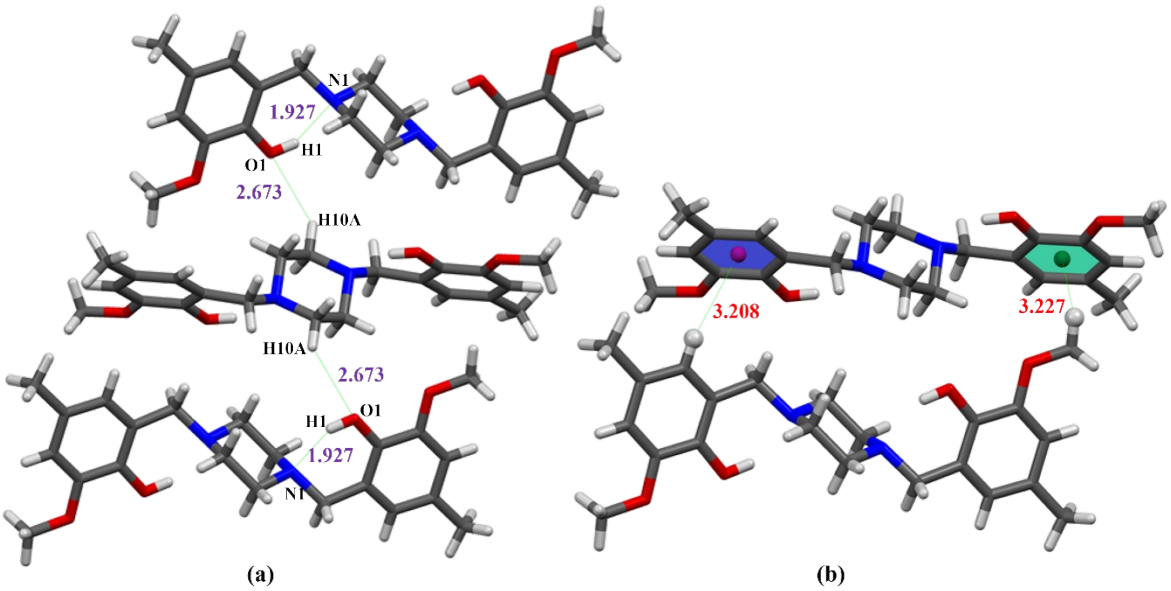

Fig. S10. **(a)** view of classical and non-classical H-bonding present in H_2L. **(b)** C-H···p interactions between the molecular units of ligand (H_2L).

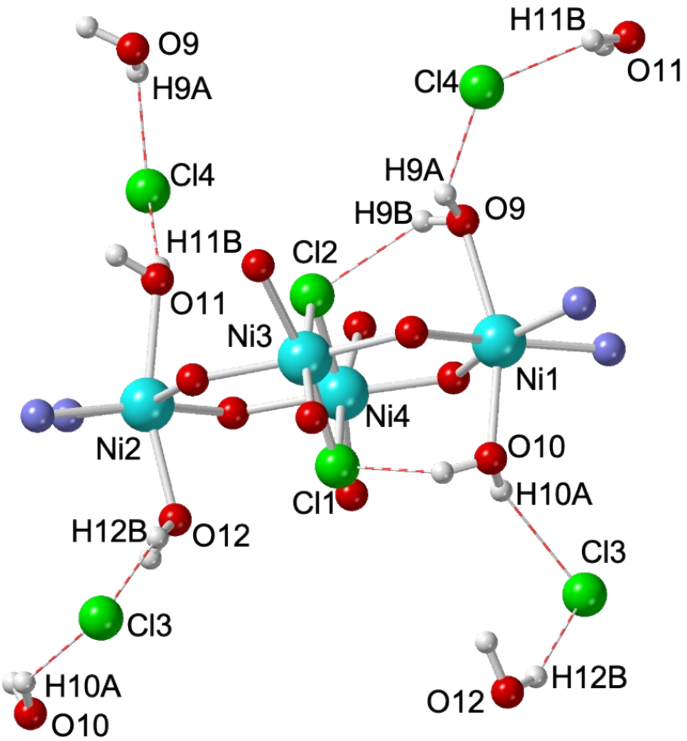

Fig. S11. Intra and intermolecular H-bonds in compound **1** (represented as dotted white and red thin lines). Only the central Ni_4 cluster and the atoms involved in the H-bonds are shown.

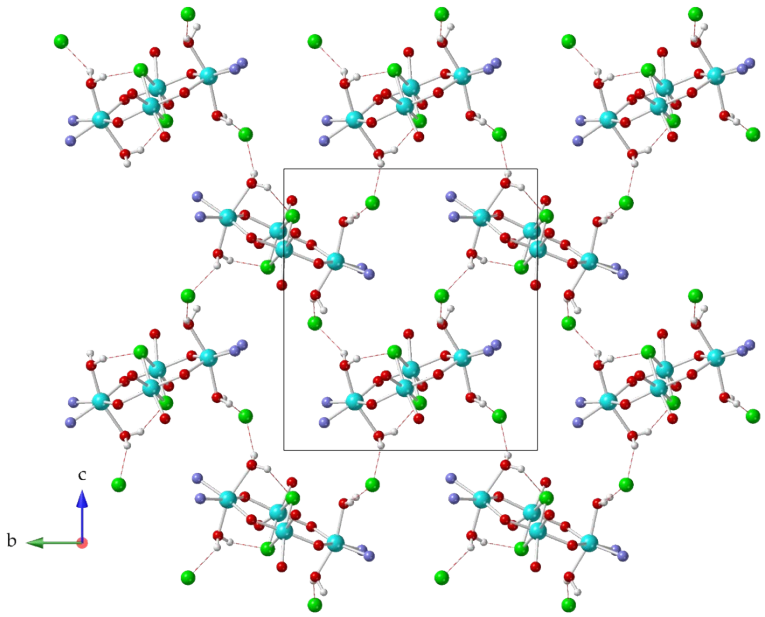

Fig. S12. Projection down the *bc* plane showing the connections of the Ni_4 complexes with four neighbouring Ni4 cluster. H-bonds are represented as dotted white and red thin lines). Only the central Ni_4 cluster and the atoms involved in the H-bonds are shown.

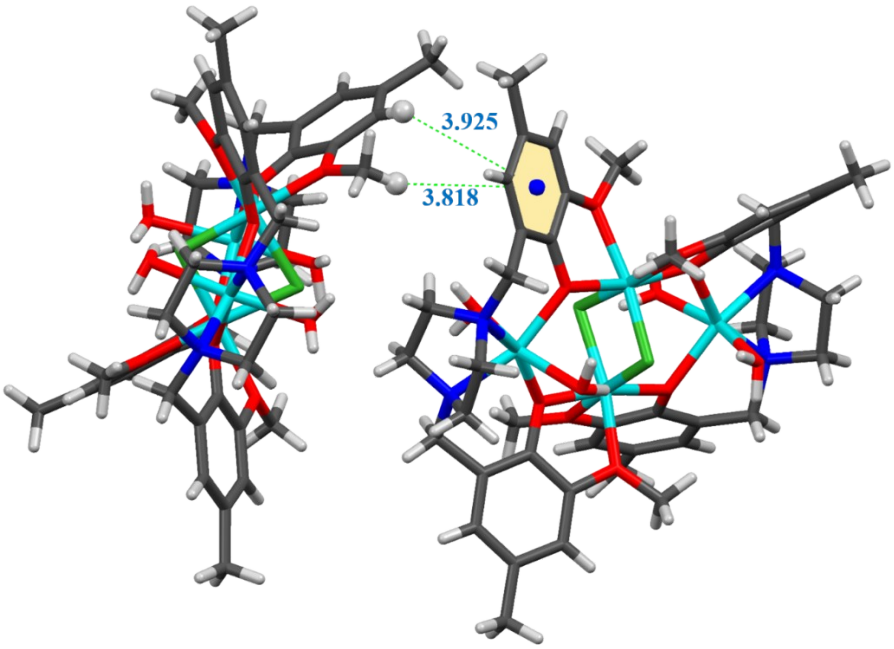

Fig. S13. View of extensive C-H···pi interactions between the molecular units of compound **1.**

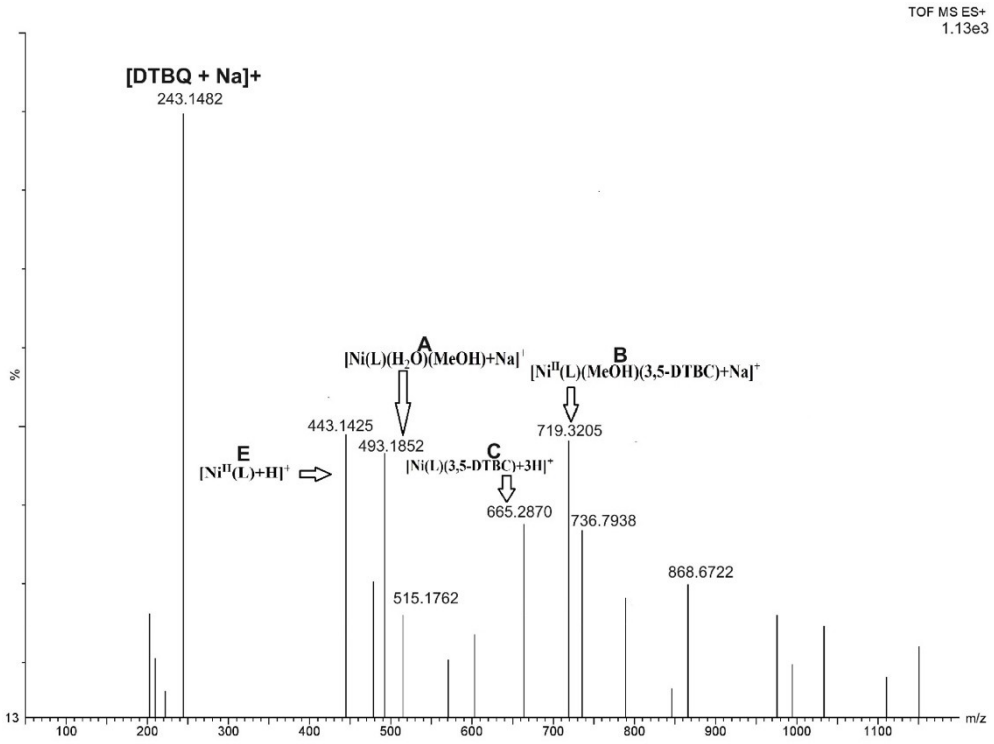

Fig. S14. Representative ESI mass spectrum of compound **1** after addition of 3,5-DTBC. (full range)

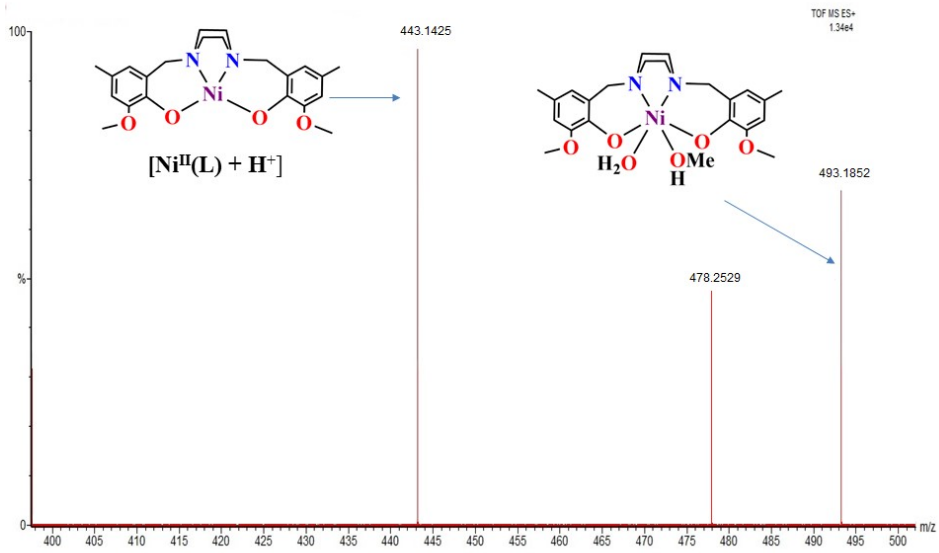

Fig. S15. Representative ESI mass spectrum of compound **1** after addition of 3,5-DTBC. (expanded from 400-500)

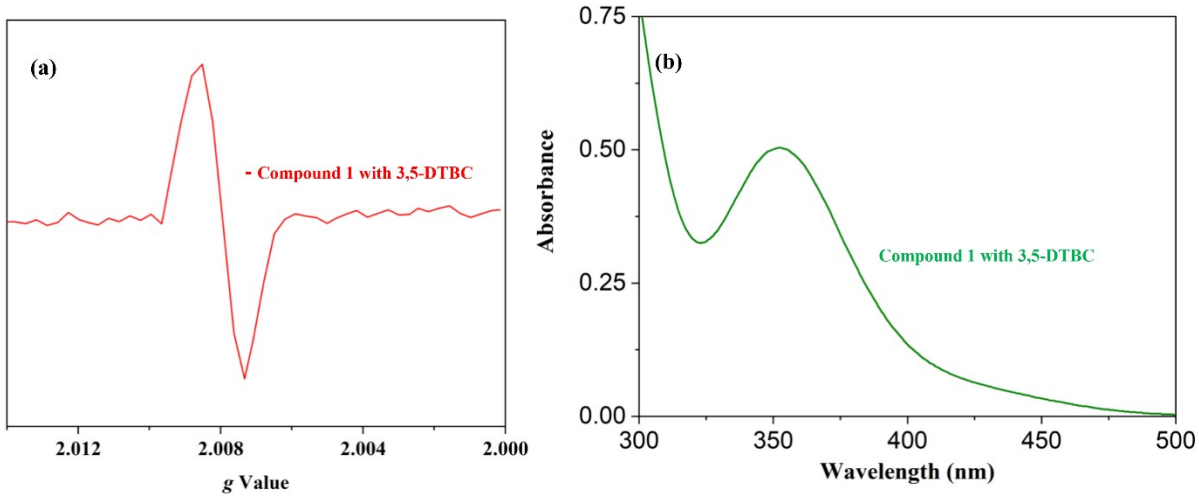

Fig. S16. (a) EPR spectrum of compound **1** with 3,5-DTBC at 110 K. **(b)** Absorption band at around 353 nm during H_2O_2 estimation(right).

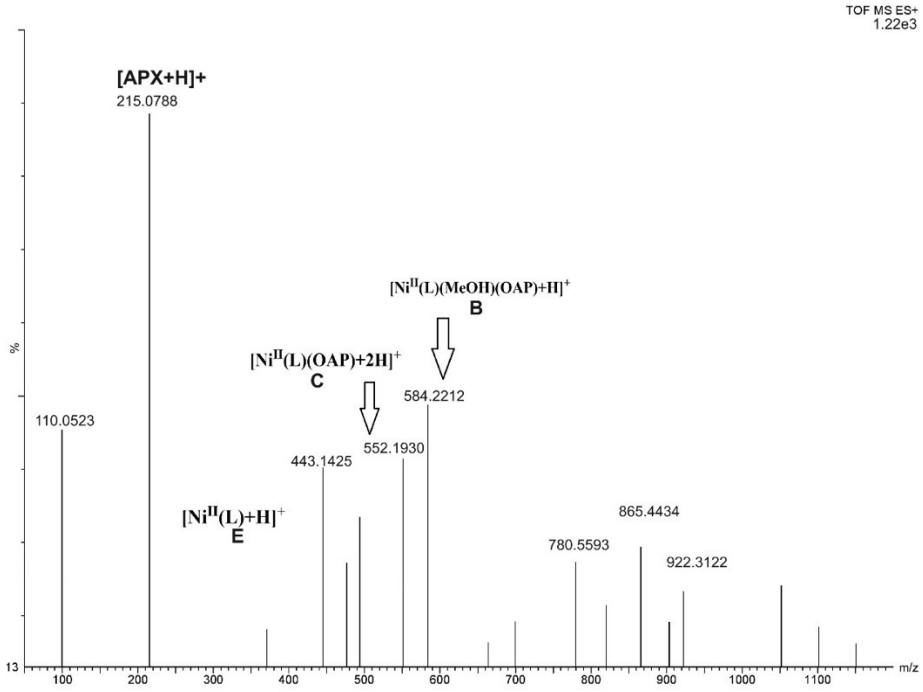

Fig. S17. ESI mass spectrum of compound **1** after addition of **OAP.**

Table S7. Kinetic parameters for the oxidation of 3,5-DTBC and *o*-aminophenol catalysed by compound **1**.

Substrate	**3,5-DTBC**	***o*-aminophenol**
V_{max} (M sec^{-1})	$3.2(4)x10^{-7}$	$2.6(3)x10^{-7}$
K_M (M)	$3.0(2)x10^{-4}$	$2.5(3)x10^{-4}$
k_{cat} (h^{-1})	28.32	17.52

Table S8. Catecholase activities of various 3d Transition metal complexes:

Metal	**Complexes**	**Solvent**	**k_{cat}(h^{-1})**	**Ref.**
Mn	$[Mn^{II}(HL^{39})(H_2O)_2(CH_3CN)](ClO_4)_2$	DMF	48.8	7
	$[Mn^{II}(L^{40})_2(H_2O)_2]$	Methanol	598	8
	$[Mn^{II}(o\text{-}(NO_2)\text{-}C_6H_4COO)_2(L^{42})(H_2O)]_n$	Acetonitrile	177.0	9
	$Mn^{III}(L^{41})(OAc)(OCH_3)]^+$	Acetonitrile	86	10
	$Mn^{III}L^{84}(SCN)(H_2O)]$	Acetonitrile	134	11
Co	$[Co^{III}Co^{II}L^{22}(N_3)_3$	Acetonitrile	114.24	12
	$[Co^{III}_2Co^{II}L^{89}R^2(MeOH)_2(N_3)_3(m_{1,3}\text{-}N_3)_3]$	Acetonitrile	99	13
	$[Co^{III}_2Co^{II}L^{89}_2(MeOH)_2(N_3)_2(m_{1,1}\text{-}N_3)_2]$	Acetonitrile	85	13
	$[Co^{III}L^{87}(NCS)_2(H_2O)]$	DMF	11.2	14
	$[Co^{III}L^{87}(N_3)_2(H_3O)^+]$	Acetonitrile	10	14
	$[Co^{II}_2(L^{35})(Cl)_2]^+$	Methanol	7.02	15
Ni	$[NiL^{76}(H_2O)_3]I_2$	methanol	92.7	16
	$[NiL^{76}(H_2O)_3]Br_2$	methanol	84.8	16
	$[Ni_2(L^{93})_2(NCS)_2]$	acetonitrile	81.7	17
	$[Ni_2(L^{91})_2(NCS)_2]$	acetonitrile	64.1	17
	$[Ni_2(L^{92})_2(NCS)_2]$	acetonitrile	51.1	17
	$[\{NiL^{89}(EtOH)\}_2Mn(NO_2)_2]$	methanol	25.8	18

	$[(NiL^{89})_2Mn(NCO)_2]$	methanol	77	13
	$[Ni(L')(H_2O)_3]^{2+}$	methanol	52.6	19
	$[Ni_2((L\text{-}(CH_3)_4)_2(H_2O)_4]^{2+}$	methanol	47.4	20
	$[\{Ni(deen)(H_2O)\}_2(\mu_3\text{-}OH)_2\text{-}\{Ni_2(moda)_4\}](ClO_4)_2\cdot 2CH_3CN$	acetonitrile	278	6
	$[\{Ni(dmpn)(CH_3CN)\}_2(\mu_3\text{-}OH)_2\{Ni_2(moda)_4\}](ClO_4)_2\cdot CH_3CN$	acetonitrile	300	6
	$[Ni_4L_2(\mu_2\text{-}Cl)_2Cl_2]$	methanol	28.32	This Work
Cu	$[Cu(L_{20})(Cl)](BF_4)$	Acetonitrile	480	21
	$[Cu(L_{21})I_2]$	DMF	63.72	22
	$[Cu(H_2L_{22})(ClO_4)]^+$	Methanol	58.68	23
	$[Cu_2(L_{13})_2]$	Methanol	720	24
	$[Cu_2(L_{12})_2(2\text{-hydroxybenzoate})_2]$	Methanol	698	25
	$[Cu_2(L_{14})_2(4\text{-hydroxybenzoate})_2][Cu(Htea)_2]$	Methanol	553	25
	$[Cu_3(\mu\text{-}OH)(dppi)_3(L_5)_3]$	THF	16.2	26
	$[Cu_3L^6{}_2](ClO_4)_2\cdot 5H_2O$	C_2H_5OH/H_2O	9.54	27
	$[Cu_3(L^7)(CH_3COO)_3].\ 3H_2O$	Methanol	7.5	28
	$[Cu^{II}{}_2(L^1)_2(NCO)_2]$	Methanol	64.2	29
	$[Cu^{II}L^3(NCO)]$	Methanol	23.6	30
	$[Cu^{II}(L^4)bpy]ClO_4$	Methanol	83.5	31
	$[Cu^{II}(L^4)phen]ClO_4$	Methanol	73.5	31
	$[Cu^{II}\ 2L^{16}(H_2O)_4](ClO_4)_4\cdot 2H_2O$	Methanol	63.0	32
	$[Cu^{II}{}_2(H_2L^{17})(ClO_4)](ClO_4)$	Methanol	58.6	32

	$[Cu_2(L^1O)$ (m-OH)] $[ClO_4]_2$	Acetonitrile	5470	33
	$[Cu_2(L^{2'}O)$ (m-OH)] $[ClO_4]_2$	Acetonitrile	163	33
	$[Cu_2(L^{3'}O)$(m-$C_3H_3N_2)(OClO_3)(H_2O)][ClO_4]\cdot H_2O$	Acetonitrile	103	33
	$[Cu_2(L^{4'})$ (m-$OH)_2]$ $(ClO_4)_2\cdot H_2O$	Acetonitrile	100	33

L^{39} = 1,3- Bis(6′-methyl-2-pyridylimino)isoindoline; L^{40} = 3-methoxy-4-hydroxy-benzaldehyde; HL^{41} = 4-tertbutyl-2,6-bis-[(2-pyridin-2-yl-ethylimino)-methyl]-phenol; L^{42} = Pyrazine; L^{84} = 2,6 diformyl-4-isopropyl phenol; L^{22} =N,N-[bis-(2-hydroxy-3-formyl-5-methylbenzyl) (dimethyl)]-ethylenediamine.]; L^{89} = N,N′-bis(salicylidene)- 1,3-propanediamine ; L^{87}= (1Z,1'Z)-N,N'-(ethane-1,2-diyl)bis(1-(3-ethoxyphenyl)methanimine); L^{35}= N,N,N' ,N' - tetrakis(20 -benzimidazolylmethyl)-1,4- diethylene amino glycol ether; L^{76}= (E)-2-(((2-(piperazin-1-yl)ethyl)imino)methyl)phenol; L^{93} = 2-[1-(3-dimethylamino-propylamino)-ethyl]-phenol; L^{91} = 2-[1-(3- methylamino-propylamino)-ethyl]-phenol; L^{92}= 2-[1-(2-dimethylamino-ethylamino)-ethyl]-phenol; L^{20} = propylene sulfide and di-(2-pyridylmethyl) amine; L^{21} =1,3-bis(20-pyridylimino)isoindoline; L^{12} = diethanolamine; L^{13} = N,N -(ethane-1,2-diyldi-ophenylene)-bis(pyridine-2-carboxamidide); L^{14} = triethanolamine; L^5 = hexafluoro acetyl acetonate and dppi = diphenylphosphinate ; L^2 = N,N-bis(3,5-dimethyl-2-hydroxybenzyl)-N',N'-dimethyl-1,2-diaminoethane;; L^7 =2,6-diformaldehyde-pyridine; HL^1 = 2-dimethylamino-ethylamino)-methyl]-phenol; HL^3 = 2-methoxy-6-(8-iminoquinolinyl-methyl)phenol; HL^4 = 2-[(3-methylamino-propylimino)-methyl]phenol; L^{16} = 2,8-dimethyl-5,11-bis(pyridin-2-ethyl)-1,4,5,6,7,10,11,12-octahydroimidazo-[4,5-h]-imidazo-[4,5c] [1,6]-diazecine; H_2L^{17} = N,N′-bis{(2-hydroxy-3-formyl-5-methylbenzyl)(dimethyl)}-ethylenediamine.

Table S9. Comparison table for phenoxazinone synthase like activities of various 3d Transition metal complexes.

Metal	Complexes	Solvent	k_{cat} (h^{-1})	Ref.
Co	$[Co_3L_2(\mu_2\text{-}C_6H_5CO_2^-)_2(CH_3CN)_2](ClO_4^-)_2\cdot(CH_3CN)_3$	methanol	7.38	34
	$[Co_3L^R{}_2(\mu_2\text{-}C_6H_5CO_2^-)_2(C_6H_5CO_2^-)_2]\cdot(CH_3CN)_2$	methanol	153.60	34
	$[Co_3L^R{}_2(\mu_2\text{-cinnamato})_2(\text{cinnamato})_2]\cdot((CH_3)_2CO)_2$	methanol	4.10	34
	$[Co_2(L^1)_2(\mu\text{-}O_2)](ClO_4)_4\cdot 2CH_3CN$	methanol	30.09	35
	$[Co_2(L^2)_2(\mu\text{-}O_2)](ClO_4)_4$	methanol	23.04	35
	$[Co(L^3)(H_2O)](ClO_4)_2$	methanol	8.28	35
	$[Co(L^4)(H_2O)](ClO_4)_2]$	methanol	6.37	35
	$[Co_2(amp)_2(\mu\text{-imp})_2Cl_2]Cl_2\cdot 2H_2O$ (1)	methanol	13.75	36
Mn	$[Mn(6'\ Me_2indH)(H_2O)_2(CH_3CN)](ClO4)_2$	DMF	2.916	7
	$[Mn(L^{169})Cl_2]$	methanol	11.88	37
	$[Mn(L^{170})Cl_2]$	methanol	9.72	37
	$[Mn(L^{171})Cl_2]$	methanol	8.28	37
	$[Mn(L^{172})Cl_2$	methanol	26.28	37
Ni	$[Ni(L)_2(DMSO)_2]$	DMSO	63.11	38
	$Ni(LH)_2(ClO_4)_2$	acetonitrile	21.4	39
	$Ni(LH)_2\ (ClO_4)_2$	methanol	202	39
	$[Ni_4L_2(\mu_2\text{-}Cl)_2Cl_2]$ (1)	methanol	17.52	This work

Cu	$[Cu^{II}{}_8O(tbdea)_6(H_2O)_2](BF_4)_2 \cdot 3CH_3OH$	methanol	2.7×10^{-6}	40
	$[Cu^{II}{}_8O(tbdea)_5(Htbdea)Cl_2][CuICl_2] \cdot 2H_2O$	methanol	7.9×10^{-5}	41
	$[Cu(ca)_2(Hbae)_2]$	methanol	4.68×10^{-4}	42
	$[Cu(va)_2(Hbae)_2]$	methanol	2.52×10^{-5}	42
	$[Cu_4(va)_4(bae)_4] \cdot H_2O$	methanol	1.44×10^{-5}	42
	$[CuI\ (CH_3CN)_2](PF_6)$	methanol	3.1×10^{-5}	42
	$[Cu(ca)_2(Hbae)_2]$	methanol	4.68×10^{-4}	42

L= *N*,*N*′-bis(salicylidene)-1,3-propanediamine; L^R= Reduced L; L^3 = N-(3-((6-methylpyridin-2-yl) methyleneamino)propyl)-N1 -methyl-N3 -((6-methylpyridin-2-yl)methylene)propane-1,3- diamine; L^4 = N- (3-((6-methylpyridin-2-yl)methyleneamino)propyl)-N-((6-methylpyridin-2-yl)methylene)pro -pane-1,3-diamine; amp= 2-aminomethylpyridine; imp= = 2-iminomethylpyridine anion]; L^{169}= (Z)-1-(pyridin-2-yl)-N-(2-(2-(pyridin-2-yl)tetrahydropyrimidin-1(2H)-yl)ethyl)methanimine; L^{170}= N-(methoxy(pyridin-2-yl)methyl)-2-(2-(pyridin-2-yl)imidazolidin-1-yl)ethan-1-amine; L^{171} = (Z)-1-(6-methylpyridin-2-yl)-N-(2-(2-(6-methylpyridin-2-yl)imidazolidin-1-yl)ethyl)methanimine; L^{172}= 2-(pyridin-2-yl)-1-(2-(2-(pyridin-2-yl)piperidin-1-yl)ethyl)hexahydropyrimidine; LH = 2-[(phenyl-pyridine-2-yl-methylene)-amino]-ethanol]; tbdea = Tercbutyl diethanolamine; Hbae = 2-benzylaminoethanol; ca = cinnamic acid; va = valeric acid.

Electrochemical measurements

Electrochemical studies of water splitting reactions were carried out with a CHI6057D electrochemical workstation usign a three electrode system which included glassy carbon, Pt wire (CHI1204) and saturated Hg/HgO as the working electrode (0.0706 cm^2), auxiliary electrode, and reference electrode respectively, using N_2 saturated 1 M KOH electrolyte. Without using any kind of binder, 2 mg of compound **1** were dispersed in 600 μL of isopropanol and sonicated for 30 min to create a homogeneous ink for coating the working electrode. Then 10 μL ink was dripped onto a glassy carbon electrode and allow to dry at room temperature. The potential values measured in our experimental setup were calculated with the reference electrode Hg/HgO and using the Nernst equation S1, that relates the measured potential with respect to the reference electrode and the RHE.

$$E_{(RHE)} = E_{(Hg/HgO)} + 0.05916 * pH + E^0_{(Hg/HgO)} \quad (S1)$$

$E_{(RHE)}$ is the reversible hydrogen electrode potential; $E_{(Hg/HgO)}$ is the experimentally measured potential with respect to the Hg/HgO electrode and $E^0_{(Hg/HgO)}$ is the standard electrode potential of the Hg/HgO electrode. The pH of the solution is 13.0 for 1 M KOH. The OER and HER LSV measurements were performed within the potential range 1.2 to 1.9 V (vs. RHE) and 0 to -1.0 V (vs. RHE), respectively, at scan rate of 5 mV s^{-1}. All the polarization curves were iR-corrected with the solution resistance (R_s) of compound **1**, measured by Electrochemical Impedance Spectroscopy (EIS) using the (E-I*Rs) relation. EIS tests were conducted in the frequency range 10^{-2} to 10^5 Hz at 1.68 V (vs. RHE) and -0.7 V (vs. RHE) for OER and HER, respectively. The Amperometric i-t experiments were performed with a current density of 10 mA cm^{-2} for OER and 30 mA cm^{-2} for HER, in order to check for the stability of the solutions.

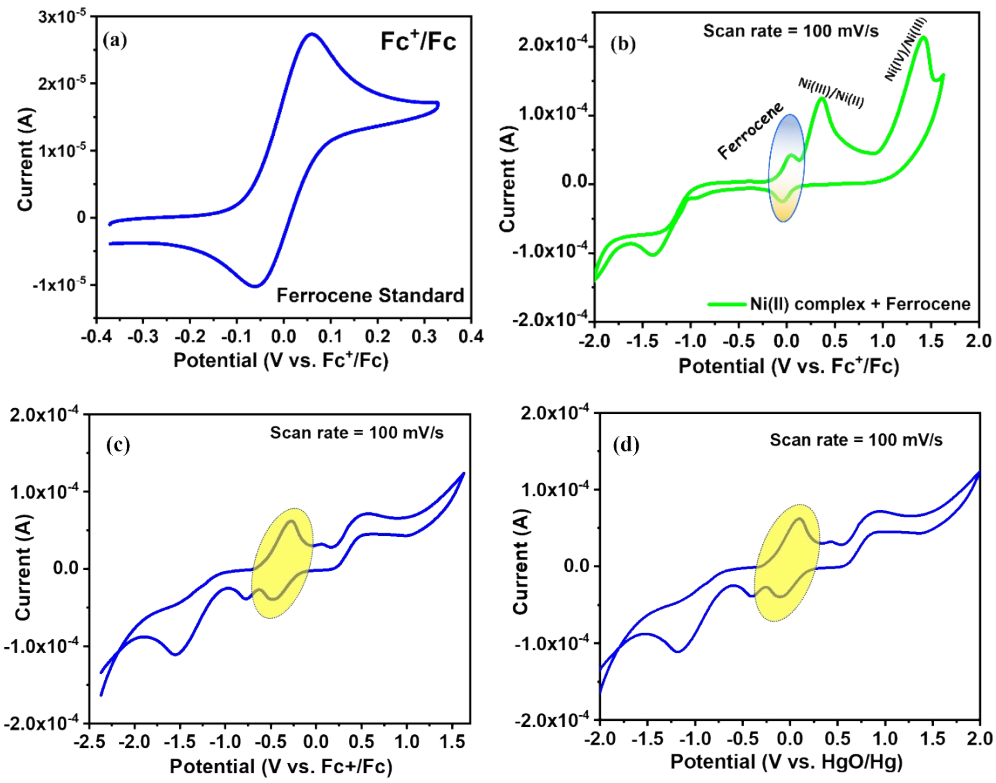

Fig. S18. Cyclic Voltammogram (CV) of **(a)** Ferrocene standard, **(b)** compound **1** + Ferrocene **(c)** only 3,5-DTBC *vs.* Fc^{+}/Fc **(D)** only 3,5-DTBC *vs.* HgO/Hg .

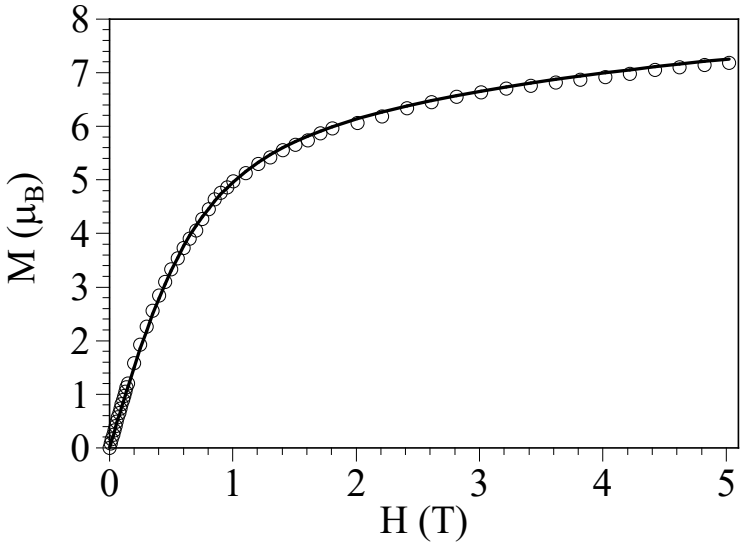

Fig. S19. Isothermal magnetization at 2 K for compound **1**. Solid line is the best fit to the model (see text).

References

(1) G. A. Bain and J. F. Berry, *J. Chem. Educ.,* 2008*,* **85**, 532-536.

(2) G. M. Sheldrick, University of Göttingen, Germany, 1997.

(3) G. M. Sheldrick, University of Göttingen, Germany, **1997**.

(4) A. L. Spek, *J. Appl. Cryst*., 2003, **36**, 7-13.

(5) O. V. Dolomanov, L. J. Bourhis, R. J. Gildea, J. A. K. Howard and H. Puschmann, *J. Appl. Crystallogr*., 2009, ***42***, 339-341.

(6) L. K. Das, A. Biswas, J. S. Kinyon, N. S. Dalal, H. Zhou and A. Ghosh, *Inorg. Chem*., 2013, ***52***, 11744-11757.

(7) J. Kaizer, G. Baráth, R. Csonka, G. Speier, L. Korecz, A. Rockenbauer and L. Párkányi, *J. Inorg. Biochem*., 2008, **102**, 773-780.

(8) S. C. Kumar, A. K. Ghosh, J. D. Chen and R. Ghosh, *Inorg. Chim. Acta*., 2017, **464**, 49-54

(9) P. Kar, Y. Ida, T. Kanetomo, M. G. B. Drew, T. Ishida and A. Ghosh, *Dalton Trans*., 2015, **44**, 9795-9804.

(10) M. U. Triller, D. Pursche, W-Y. Hsieh, V. L. Pecoraro, Annette. Rompel and Bernt. Krebs, *Inorg. Chem.,* 2003, **42***,* **20**, 6274-6283.

(11) M. Maiti, D. Sadhukhan, S. Thakurta, E. Zangrando, G. Pilet, A. Bauzá, A. Frontera, B. Dede and S. Mitra, *Polyhedron.,* 2014, **75,** 40-49.

(12) L. Mandal, S. Sasmal, H. A. Sparkes, J. A. K. Howard and S. Mohanta, *Inorg. Chim. Acta*., 2014, **412**, 38-45.

(13) A. Hazari, L. K. Das, R.M. Kadam, A. Bauza, A. Frontera and A. Ghosh, *Dalton Trans.*, 2015, **44***,* 3862-3876.

(14) P. Chakraborty and S. Mohanta, *Inorg. Chim. Acta.,* 2015, **435**, 38-45.

(15) J.-H. Qiu, Z.-R. Liao, X.-G. Meng, L. Zhu, Z.-M. Wang and K.-B. Yu, *Polyhedron*., 2005, **24**, 1617-1623.

(16) P. Adhikary Chakraborty, S. Das, T. Chattopadhyay, A. Bauza, S.K. Chattopadhyay, B. Ghosh, F. A. Mautner, A. Frontera and D. Das, *Inorg. Chem*., 2013, **52***,* **23***,*13442-13452.

(17) A. Biswas, L. K. Das, M. G. B. Drew, G. Aromi, P. Gamez and A. Ghosh, *Inorg. Chem.,* 2012, **51**, **15**, 7993-8001.

(18) P. Seth, L. K. Das, M. G. B. Drew and A. Ghosh, *Eur. J. Inorg. Chem.,* 2012, 2232-2242.

(19) A. Guha, K. S. Banu, S. Das, T. Chattopadhyay, R. Sanyal, E. Zangrando and D. Das, *Polyhedron*, 2013, **52**, 669-678.

(20) A. Guha, A. Banerjee, R. Mondol, E. Zangrando and D. Das, *J. Coord. Chem.,* 2011, **64**, 3872-3886.

(21) E. C. M. O-Wenker, M. A. Siegler, M. Lutz and E. Bouwman, *Dalton Trans*., 2015, **44**, 12196-12209.

(22) Á. Kupán, J. Kaizer, G. Speier, M. Giorgi, M. Réglier and F. Pollreisz, *J. Inorg. Biochem*., 2009, **103**, 389-395.

(23) T. P. Camargo, R. A. Peralta, R. Moreira, E. E. Castellano, A. J. Bortoluzzi and A. Neves, *Inorg. Chem. Commun*., 2013, **37**, 34-38.

(24) S. Sarkar, A. Sim, S. Kim and H. I. Lee, *J. Mol. Catal. A: Chem*., 2015, **410**, 149-159.

(25) F. Sama, A. K. Dhara, M. N. Akhtar, Y.-C. Chen, M.-L. Tong, I. A. Ansari and M. Raizada, *Dalton Trans***.,** 2017,**46**, 9801-9823.

(26) S. Calancea, S. G. Reis, G. P. Guedes, R. A. A. Cassaro, F. Semaan, F. L. Ortiz and M. G. F. Vaz, *Inorg. Chim. Acta*, 2016, **453**, 104-114.

(27) A. Szorcsik, F. Matyuska, A. Bényei, N. V. Nagy, R. K. Szilágyie and T. Gajda, *Dalton Trans*., 2016, **45**, 14998-15012.

(28) V. K. Bhardwaj, N. A. Alcalde, M. Corbella and G. Hundal, *Inorg. Chim. Acta*., 2010, **363**, 97-106.

(29) A. Biswas, L. K. Das and A. Ghosh, *Polyhedron*., 2013, **61**, 253–261.

(30) M. Shyamal, T. K. Mandal, A. Panja and A. Saha, *RSC Adv*., 2014, **4**, 53520-53530.

(31) A. Bhunia, P. Vojtısek and S. C. Manna, *J. Mol. Struct*., 2019, **1179**, 558-567.

(32) M. R. Mendoza-Quijano, G. Ferrer-Sueta, M. Flores-Álamo, N. Aliaga-Alcalde, V. Gómez-Vidales, V. M. Ugalde Saldívara and L. Gasque, *Dalton Trans*., 2012, **41**, 4985-4997.

(33) J. Mukherjee and R. N. Mukherjee, *Inorg. Chim. Acta.,* 2002, **337**, 429-438.

(34) A. Hazari, A. Das, P. Mahapatra and A. Ghosh, *Polyhedron*., 2017, **134**, 99-106.

(35) A. Panja, *Dalton Trans.,* 2014, **43**, 7760-7770.

(36) A. Panja and P. Guionneaua, *Dalton Trans*., 2013, **42**, 5068-5075.

(37) A.Panja, *Polyhedron.,* 2014, **79**, 258-268.

(38) S. Sengupta, S. Khan, S. K. Chattopadhyay, I. Banerjee, T. K. Panda and S. Naskar, *Polyhedron*, 2020, **182**, 114512.

(39) A. Chatterjee, S. Khan and R. Ghosh, *Polyhedron,* 2019, **173**, 114151.

(40) D. S. Nesterov, V. N Kokozay, V. V. Dyakonenko, O. V. Shishkin, J. Jezierska, A. Ozarowski, A. M. Kirillov, M. N. Kopylovich and A. J. L. Pombeiro, *Chem. Commun*., 2006, 4605-4607.

(41) P. Seppala, R. Sillanpaa and A. Lehtonen, *Coord. Chem. Rev*., 2017, **347**, 98-114.

(42) O. V. Nesterova, O. E. Bondarenko, A. J. L. Pombeiro and D. S. Nesterov, *Dalton Trans.*, 2020, **49**, 4710-4724.